# Predictive analysis for triton burnup ratio in HL-2A and HL-2M plasmas



# Predictive analysis for triton burnup ratio in HL-2A and HL-2M plasmas

Kunihiro Ogawa[1,2], Yipo Zhang[3], Jie Zhang[3], Siriyaporn Sangaroon [1,4], Mitsutaka Isobe[1,2], and Yi Liu[3]

[1]*National Institute for Fusion Science, National Institutes of Natural Sciences, Toki, Japan*

[2]*The Graduate University for Advanced Studies, SOKENDAI, Toki, Japan*

[3]*Southwestern Institute of Physics*, Chengdu, China

[4]*Faculty of Science, Mahasarakham University, Maha Sarakham, Thailand*

Abstract

The expected triton burnup ratio was analyzed based on numerical simulation to study the feasibility of demonstrating energetic particle confinement through 1 MeV triton burnup experiments in HL-2A and HL-2M. Calculations were conducted using LORBIT, a collisionless Lorentz orbit code, and FBURN, a neutron emission calculation code based on the classical confinement of energetic particles. First, the orbit loss and radial distribution of the tritons were evaluated using the LORBIT code. The LORBIT code revealed that all tritons were lost within ~$10^{-6}$ s in HL-2A, whereas in HL-2M, most of the tritons were still confined at $10^{-3}$ s. The FBURN code calculated the deuterium-tritium neutron emission rate using the radial

distribution of 1 MeV tritons. The predictive analysis found that nearly no deuterium-tritium neutrons remained in HL-2A at a plasma current of 160 kA. Also, in HL-2M, a significant triton burnup ratio could be obtained at the relatively high plasma currents of 1 MA, 2 MA, and 3 MA. This analysis predicts that the triton burnup ratio exceeds one percent under relatively high plasma current conditions.

Keywords: HL-2A, HL-2M, Triton burnup, energetic particle confinement

## 1. Introduction

In a fusion reactor, a fusion burning plasma is sustained by deuterium-tritium fusion-born alpha particles with the initial energy of 3.5 MeV. Thus, the notable performance of alpha particle confinement is necessary to sustain fusion burning plasmas. The study of energetic particle confinement has been receiving much attention in confinement of beam ions, ion cyclotron frequency range heated tail ions, and fusion products in magnetic confinement fusion devices. One of the indexes that are commonly used in deuterium plasma experiments to show the performance of fusion product confinement is the triton burnup ratio, defined as the deuterium-tritium neutron yield divided by the deuterium-deuterium neutron yield. In a deuterium plasma experiment, a deuterium-deuterium reaction has two branches: D(d,n)$^3$He and D(d,p)T. These two branches have nearly identical probabilities. Therefore, the triton burnup ratio indicates the ratio of the number of

deuterium-tritium reactions on the total number of 1 MeV tritons. If the 1 MeV tritons slow down inside the plasma to approximately 100 keV, at which the deuterium-tritium reaction reaches its peak, the secondary deuterium-tritium reaction occurs. The confinement ability of 1 MeV tritons can be evaluated by quantifying the total number of deuterium-tritium reactions. The advantages of using 1 MeV tritons compared to beam ions and ion cyclotron frequency range heated tail ions are the kinetic parameter and initial velocity distribution. The 1 MeV triton's kinetic parameters, such as Larmor radii, are almost identical to the kinetic parameters of the 3.5 MeV alpha particle. The initial velocity distribution of 1 MeV tritons is isotropic, as is the initial velocity distribution of 3.5 MeV alpha particles. The triton burnup experiment has been performed in the middle to large tokamaks and a helical device [1-15]. A superior triton burnup ratio of greater than one percent was obtained in large tokamaks.

Energetic ion confinement has been studied in HL-2A using a neutron flux monitor, a radial neutron camera [16], and a fast-ion loss detector [17, 18]. The classical confinement of beam ions and the loss of beam ions due to magnetohydrodynamics instabilities were studied [19-24]. Based on the knowledge of HL-2A, energetic particle confinement studies will be performed in HL-2M using comprehensive neutron diagnostics. In this paper, predictive analyses of the triton burnup ratio in both HL-2A and HL-2M are presented. The calculation setup for the triton burnup ratio analyses is described in section 2. In section 3, the results of the analyses are presented. A summary of the paper

may be found in section 4.

## 2. Setups for triton burnup ratio calculation

The triton burnup analysis in HL-2A was performed with the plasma current $I_p$ of 160 kA. The triton burnup analysis in the HL-2M was performed at the $I_p$ values of 1 MA, 2 MA, and 3 MA, with varying plasma density. The flowchart of the calculation is shown in Fig. 1. The electron temperature profile was assumed to be parabolic $T_{e0}(1-\rho^2)$, where $T_{e0}$ and $\rho$ represent the central electron temperature and normalized minor radius, respectively. Here, the ion temperature is assumed to be the same as the electron temperature. Here, the ratio of the line-averaged electron temperature on $T_{e0}$ is 0.67. The density profile was assumed to be a relatively flat profile $n_0(1-\rho^8)$, where $n_0$ represents the central density. The plasma is assumed to be a pure deuterium plasma. $T_{e0}$ was estimated using ITERH-98P(y,2) scaling [25] (see Appendix 1). In this evaluation, all the available heating sources were considered to be the heating power. In the HL-2A case, the heating power was set to be 9.0 MW, whereas, in the HL-2M case, the heating power was set to be 25 MW. Figure 2 shows $T_{e0}$ as a function of the line-averaged density. In this analysis, the line-averaged density was increased from 2 x $10^{19}$ $m^{-3}$ to 5 x $10^{19}$ $m^{-3}$ in $10^{19}$ $m^{-3}$ increments. In HL-2A, $T_{e0}$ was changed from 0.7 keV to 1.2 keV. In HL-2M, at an $I_p$ of 1 MA, $T_{e0}$ was changed from 2.7 keV to 4.7 keV. In HL-2M, at an $I_p$ of 3 MA, $T_{e0}$ increases with $I_p$ according to the scaling law and reaches 13 keV at the line-averaged

density of 2 x $10^{19}$ $m^{-3}$. Note that the density range considered in this calculation is relatively low compared to the comprehensive simulation [26]. Because the analysis of this paper is devoted to predicting the higher triton burnup ratio condition for HL-2M, the longer slowingdown time, which corresponding to the higher temperature, is favorable. The relatively high-temperature plasmas can be obtained in relatively low-density conditions. The plasma equilibrium was given by the EFIT result. The EFIT file of shot number 36321 was used in the HL-2A case, while the predictive EFIT files were used in the HL-2M case. Note that the EFIT file was fixed for each value of $I_p$. The radial profile of the triton emissivity was calculated by following deuteron beam orbits for one second using the NUBEAM code [27]. Here, two neutral beams (NB) injectors were considered in the calculation. In the HL-2A case, the acceleration voltage of NB was set to be 40 keV, whereas, in the HL-2M case, the acceleration voltage of NB was set to be 80 keV. Based on the radial profile of the triton emissivity calculated by the NUBEAM code, 1 MeV tritons were randomly launched in position with a random number generator. The initial velocity direction was randomly provided by a random number generator. The collisionless Lorentz orbit was followed using the LORBIT code [28]. The orbit following time was set to be 1 ms, which was much shorter than a 1 MeV triton's slowing-down time, which is typically more than 100 ms. Note that the toroidal ripple was not considered in this calculation. The loss boundary of tritons was at the vacuum vessel. Deuterium-tritium neutron emission calculation was performed based on the classical confinement of 1 MeV

tritons, where the radial distribution of 1 MeV triton does not change, using the FBURN code without considering the radial diffusion [29].

## 3. Results of triton burnup ratio calculation

### 3.1 HL-2A

The radial profile of the 1 MeV triton emissivity, calculated using the NUBEAM code, is shown in Fig. 3 (a). Here, the number of radial grids is set to be 100. The emissivity has a peak at the normalized minor radius ($r/a$) of 0.2 to 0.5, which falls sharply towards the plasma edge region. The birth position of the 1 MeV triton used in the LORBIT code together with the magnetic flux surface is shown in Fig. 3 (b). The pink line indicates the wall of HL-2A. A typical 1 MeV triton orbit is shown in Fig. 4. In this calculation, the start point of the tritons was set to be ($R$, $Z$) = (1.80 m, 0.1 m), where $R$ and $Z$ represent major radius and height, respectively. In this configuration, the toroidal magnetic field and $I_p$ are directed to be from the backside to the front side of the paper. Therefore, the direction of the gradient magnetic field $B$ drift is directed to be lower. The toroidal magnetic field strength was ~1.3 T. The pitch angle of co-going, counter-going, and trapped tritons are 5 degrees, 174 degrees, and 96 degrees, respectively. In this plot, all the tritons immediately escape from the plasma and reach the HL-2A wall due to the low $I_p$. Note that the Larmor radius of the trapped triton

is almost the same as the minor radius of the HL-2A plasma. $10^5$ particles were launched according to the triton emissivity shown in Fig. 3 (b). The orbit of the triton was followed up to 1 ms using the LORBIT code. Figure 5 (a) shows the time evolutions of the confined particles as functions of time. The number of confined particles started to decrease from $t$ = ~2 x $10^{-8}$ s, nearing zero at $t$ = $10^{-6}$ s. As shown in Fig. 4, the 1 MeV tritons were almost unconfined in the HL-2A at an $I_p$ of 160 kA. The 1 MeV triton density obtained in the LORBIT calculation is shown in Fig. 5 (b). Here, the existence probability of a triton is proportional to the time spent by the triton in each radial grid. The deuterium-tritium neutron emission rate $S_{n\_DT}$ was calculated based on Fig. 5 (b) using the FBURN code. Here, the 1 MeV tritons are assumed to be continuously generated until $t$ = 3 s. The time evolution of $S_{n\_DT}$ normalized by the total DD neutron emission rate $S_{n\_DD}$, as shown in Fig. 6, represents the rapid increase of $S_{n\_DT}/S_{n\_DD}$ rapidly in time. $S_{n\_DT}/S_{n\_DD}$ reaches a substantially small final value of 3.5 x $10^{-8}$ at $t$ = 0.12 s.

### 3.2 HL-2M

The radial profile of 1 MeV triton emissivity in HL-2M, at an $I_p$ of 1 MA and the line-averaged density of 2 x $10^{19}$ $m^{-3}$, was calculated by the NUBEAM code, as shown in Fig. 7 (a). The profile has a peak at the plasma center, which falls gradually towards the plasma edge. The 1 MeV tritons were launched according to the two-dimensional triton emissivity profile shown in Fig. 7 (b). Figure 8 shows the typical triton orbit in the HL-2M at an $I_p$ of 1 MA, 2 MA, and 3 MA. The pink line

indicates the position of the HL-2M wall. In this plot, the start point is set to be ($R$, $Z$) = (1.7 m, 0.4 m). The initial pitch angles of the co-going transit, counter-going transit, and trapped tritons were 10 degrees, 168 degrees, and 88 degrees, respectively. In this calculation, the direction of the toroidal magnetic field and $I_p$ are directed to be from the front side to the backside of the paper. Therefore, the ion gradient $B$ drift is directed to be upwards. The strength of the toroidal magnetic field was ~2.2 T. At the $I_p$ of 1 MA, the co-going, as well as the counter-going transit tritons, were confined, whereas the trapped triton is lost to the wall. The orbital deviation of the co-going and the counter-going transit tritons were significant due to the high energy of the tritons. At the $I_p$ of 2 MA, the co-going and counter-going transit tritons, as well as the trapped tritons, were confined. The deviation of the orbit from the flux surface became smaller compared to the deviation at the $I_p$ of 1 MA. At the $I_p$ of 3 MA, the co-going and the counter-going transit tritons, as well as the trapped tritons, were confined. The deviation of the orbit from the flux surface became substantially small, and then the banana width became thin due to the high $I_p$. $10^5$ 1 MeV tritons were launched according to the two-dimensional distribution shown in Fig. 7 (b). Figure 9 (a) depicts the time evolution of the number of confined particles. Here, the averaged plasma density is 2 x $10^{19}$ $m^{-3}$. The number of confined particles decreased at $t$ =~$10^{-6}$ s and became constant at $t$ =$10^{-5}$ s. Note that the time evolution of the number of confined particles is similar to the time evolution evaluated for EAST plasmas [30]. The number of confined particles at the $I_p$ values of 1 MA, 2 MA, and 3 MA reached approximately

52000, 83000, and 94000, respectively. Figure 9 (b) shows the radial profile of the 1 MeV triton density obtained in the LORBIT calculation. The triton density profile is almost unchanged regardless of $I_p$. $S_{n\_DT}/S_{n\_DD}$ was calculated using the FBURN code. Figure 10 shows the time evolution of $S_{n\_DT}/S_{n\_DD}$ at the line averaged density of 2 x $10^{19}$ $m^{-3}$. At an $I_p$ of 1 MA, $S_{n\_DT}/S_{n\_DD}$ increased gradually until $t$ =~1.0 s, then $S_{n\_DT}/S_{n\_DD}$ reaches 0.30%. At an $I_p$ of 2 MA, $S_{n\_DT}/S_{n\_DD}$ increased more rapidly than at an $I_p$ of 1 MA, until $t$ =~1.5 s, and then $S_{n\_DT}/S_{n\_DD}$ reached 0.95%. At an $I_p$ of 3 MA, $S_{n\_DT}/S_{n\_DD}$ increased at almost the same rate as at an $I_p$ of 2 MA, until $t$ =~2.0 s, then $S_{n\_DT}/S_{n\_DD}$ reaches 1.4%. It is worth noting that the longer rise time of $S_{n\_DT}/S_{n\_DD}$ in higher $I_p$ case is due to the higher plasma temperature. The reached value of $S_{n\_DT}/S_{n\_DD}$ is considerably higher than the value reached in the HL-2A case.

The triton burnup ratio under each condition is summarized in Fig. 11. Here, the neutron yield was calculated by integrating $S_{n\_DT}$ or $S_{n\_DD}$, as shown in Figs. 6 and 10, respectively. In the HL-2A case, the obtained triton burnup ratio was approximately $3x10^{-8}$. The measurement of the deuterium-tritium fusion neutron is thought to be highly unfeasible because of the low number of deuterium-tritium neutrons. In the HL-2M case, the triton burnup ratio became higher in the lower density region of this calculated density range. The triton burnup ratios reach 0.29%, 0.88%, and 1.3% at the $I_p$ values of 1 MA, 2 MA, and 3 MA, respectively. The triton burnup ratio noticeably increased with the increase of $I_p$. One of the motivations behind obtaining the high triton burnup ratio is the

improvement of the 1 MeV triton confinement ability. As shown in Fig. 9 (a), the number of confined particles improved in the high $I_p$ case. The other reason for the high triton burnup ratio in the high $I_p$ case is the improvement of plasma performance, i.e., the electron temperature. As shown in Fig. 2, $T_{e0}$ increased significantly with increasing $I_p$, according to the scaling law. Tritons slowdown relatively slowly, which induces the higher possibility of deuterium-tritium fusion reactions. It was found that in the HL-2M, most of 1 MeV tritons are confined, and the triton burnup ratio has the potential to exceed one percent. A deuterium-tritium neutron detector, such as a scintillating fiber detector [10, 31-34], can be utilized to demonstrate the alpha particle confinement ability in HL-2M plasmas.

## 4. Summary

A predictive analysis of triton burnup ratio in the HL-2A and HL-2M was performed to identify the possibility of a triton burnup study in the interest of demonstrating the energetic confinement performance of both devices. Triton burnup ratio was calculated for HL-2A plasma at an $I_p$ value of 160 kA as well as for HL-2M at $I_p$ values of 1 MA, 2 MA, and 3 MA. The Lorentz orbit calculation based on the radial profile of 1 MeV triton emissivity calculated by the NUBEAM reveals that all tritons were lost within $10^{-6}$ s in the HL-2A case, whereas the number of confined tritons became constant within $10^{-5}$ s in the HL-2M case. The deuterium-tritium neutron emission calculation based

on the classical confinement of the triton shows that the triton burnup ratio is almost zero in the HL-2A, whereas, in the HL-2M, the triton burnup ratio exceeds one percent at an $I_p$ of 3 MA. It is shown that high triton confinement ability, which corresponds to the energetic alpha confinement ability, is expected in HL-2M plasmas.

Acknowledgments

This work was supported by the Japan-China Post-Core-University-Program, Post-CUP, and by the NINS program of Promoting Research by Networking among Institutions (Grant Number 01411702).

Appendix 1 Evaluation of the central temperature from the energy confinement time

Temperature and density profiles are assumed to be $T(\rho)=T_0(1-\rho^2)$ and $n(\rho)=n_0(1-\rho^8)$, respectively. Here, $T$, $\rho$, $T_0$, $n$, and $n_0$ represent temperature, normalized minor radius, the central temperature, density, the central density, respectively. The stored energy $W_p$ is expressed as

$$\mathrm{W}_p = \mathrm{W}_{pe} + \mathrm{W}_{pi} = 2 \times 2\pi R \cdot a^2 \int_0^1 2\pi\rho \mathrm{d}\rho \left[\frac{3}{2} n_0(1-\rho^8) T_0(1-\rho^2)\right]$$

$$= 12\pi^2 R a^2 n_0 T_0 \int_0^1 \rho \mathrm{d}\rho[(1-\rho^8)(1-\rho^2)],$$

where $W_{pe}$, $W_{pi}$, $R$, and $a$ indicate the stored energy of the electron, the stored energy of ion, the

major radius, and the minor radius, respectively. Letting $\rho^2$ to $\mu$ then,

$$W_p = 6\pi^2 R a^2 n_0 T_0 \int_0^1 d\mu[(1-\mu^4)(1-\mu)] = \frac{14\pi^2}{5} R a^2 n_0 T_0$$

Hence, $T_0$ in steady-state plasmas can be expressed using the elementary charge $e$ as

$$T_0 = \frac{5}{14\pi^2}\frac{W_p}{\kappa R a^2 n_0 e} = \frac{5}{14\pi^2}\frac{P\tau_E}{\kappa R a^2 n_0 e}[eV],$$

where $P$ and $\tau_E$ denote the input power and the energy confinement time, respectively. Here, the effect of plasma elongation $\kappa$ is included according to [35, 36].

References


[1] Barnes C.W. et al 1998 Nucl. Fusion **38** 597.

[2] Conroy S. et al 1988 Nucl. Fusion **28** 2127.

[3] Heidbrink W.W., Chrien R.E., and Strachan J.D. 1983 Nucl. Fusion **23** 917.

[4] Hoek M., Bosch H.-S. and Ullrich W. 1999 Triton burnup measurements at ASDEX Upgrade by neutron foil activation IPP-Report IPP-1/320.

[5] Batistoni P et al 1987 Nucl. Fusion **27** 1040.

[6] Duong H.H. and Heidbrink W.W. 1993 Nucl. Fusion **33** 211.

[7] Nishitani T. et al 1996 Plasma Phys. Control. Fusion **38** 355.

[8] Jungmin J. et al 2016 Rev. Sci. Instrum. **87** 11D828.

[9] Jungmin J. et al 2018 Rev. Sci. Instrum. **89** 11I118.

[10] Ogawa K. et al 2018 Nucl. Fusion **58** 034002.

[11] Ogawa K. et al 2019 Nucl. Fusion **59** 076017.

[12] Pu N. et al, 2018 Rev. Sci. Instrum. **89** 10I105.

[13] Pu N. et al 2018 Plasma Fusion Res. **13** 3402121.

[14] Isobe M. et al 2018 IEEE Trans. Plasma Sci. **46** 2050.

[15] Isobe M. et al 2018 Nucl. Fusion **58** 082004.

[16] Zhang Y. P. et al 2016 Rev. Sci. Instrum. **87** 063503.

[17] Zhang Y. P. et al 2014 Rev. Sci. Instrum. **85** 053502.

[18] Isobe M. et al 2017 Fusion Sci. Technol. **72** 60.

[19] Isobe M. et al 2009 Chin. Phys. Lett. **26** 105201.

[20] Isobe M. et al 2011 Plasma Fusion Res. **6** 2402107.

[21] Zhang Y. P. et al 2012 Phys. Plasmas **19** 1120504.

[22] Liu Yi et al 2012 Nucl. Fusion **52** 074008.

[23] Zhang Y. P. et al 2015 Nucl. Fusion **55** 113024.

[24] Xu M. et al 2015 Nucl. Fusion **55** 104022.

[25] ITER Physics Basis 1999 Nucl. Fusion **39** 2175 (chapter 2, section 6.3.1.).

[26] Xue L. et al 2020 Nucl. Fusion **60** 016016.

[27] Pankin A. et al 2004 Comput. Phys. Commun. **159** 157.

[28] Isobe M. *et al* 2009 J. Plasma Fusion Res. SERIES **8** 330.

[29] Ogawa K. et al 2018 Plasma Phys. Control. Fusion **60** 095010.

[30] Ogawa K. et al 2020 Plasma Fusion Res. **15** 2402022.

[31] Ogawa K et al 2018 Rev. Sci. Instrum. **89** 10I101.

[32] Takada E. et al 2019 Rev. Sci. Instrum. **90** 043503.

[33] Pu N. et al 2019 J. Instrum. **14** P10015.

[34] Pu N. et al 2020 Nucl. Instrum. Meth. Phys. Res. A **969** 164000.

[35] Sarazin Y. et al 2020 Nucl. Fusion **60** 016010.

[36] Johner J. 2011 Fusion Sci. Technol **59 2** 308.

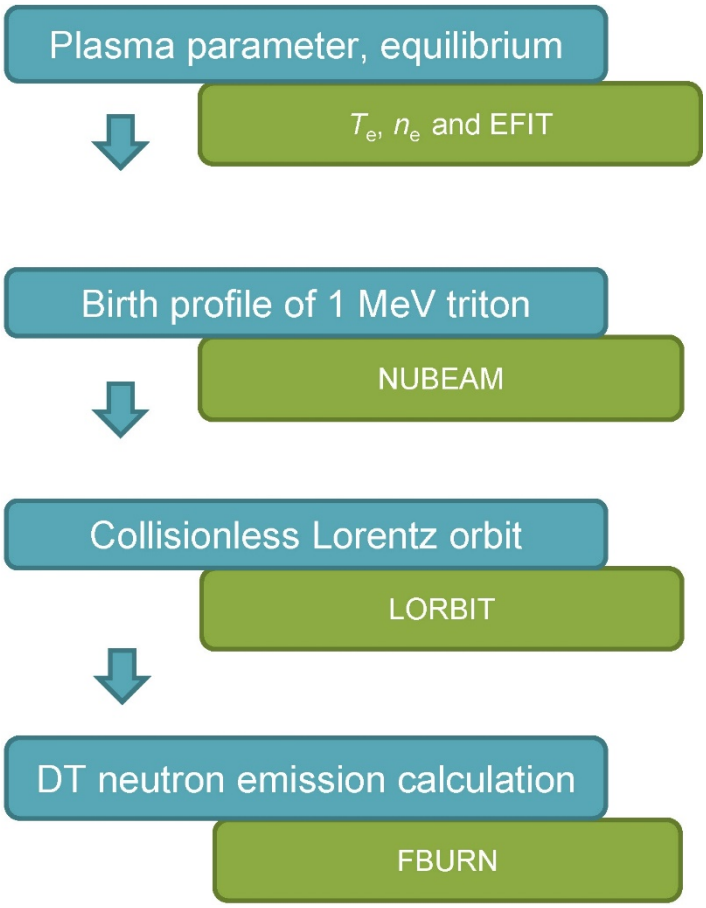


Fig. 1 Flowchart of triton burnup predictive analysis.

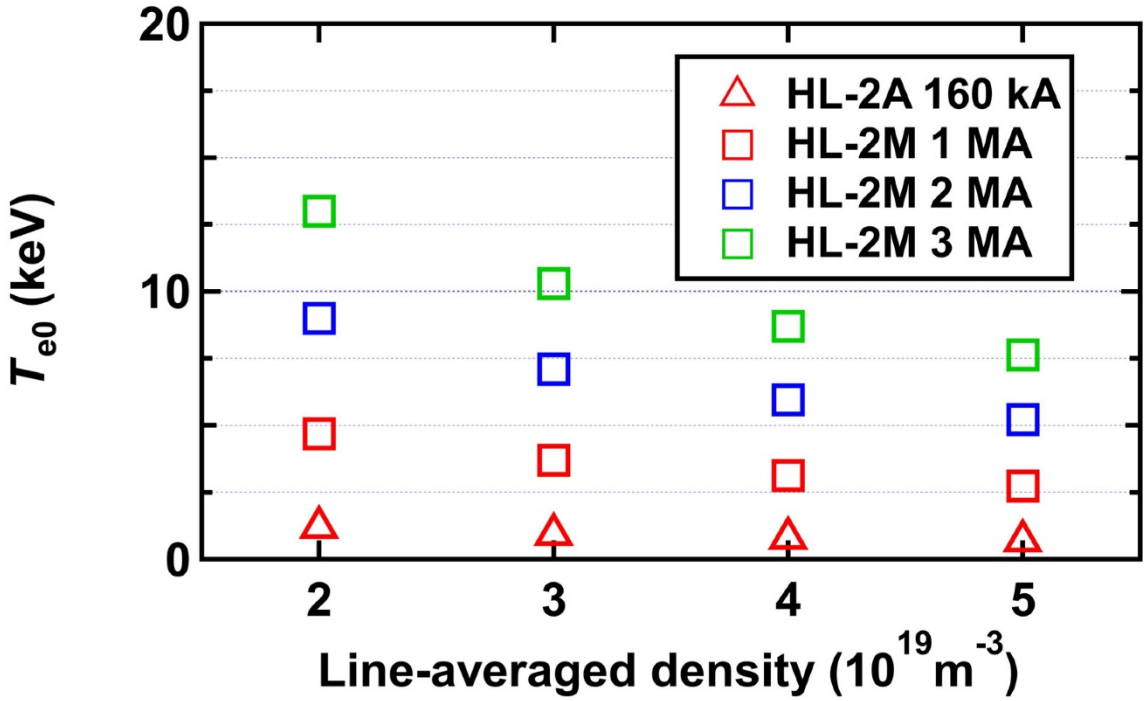


Fig. 2 Central electron temperature estimated based on ITERH-98P(y,2) scaling.

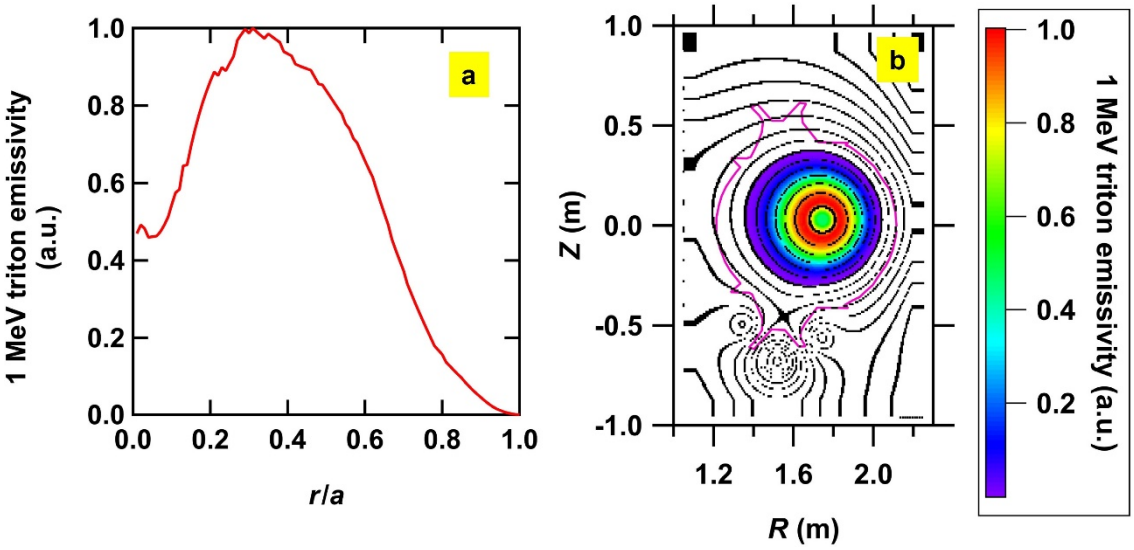


Fig. 3 (a) Radial profile of 1 MeV triton emissivity calculated by the NUBEAM code for the HL-2A, with an $I_p$ of 160 kA with the line-averaged density of 2 x $10^{19}$ $m^{-3}$. (b) Two-dimensional plot of the birth profile of a 1 MeV triton in HL-2A, as used in the LORBIT code.

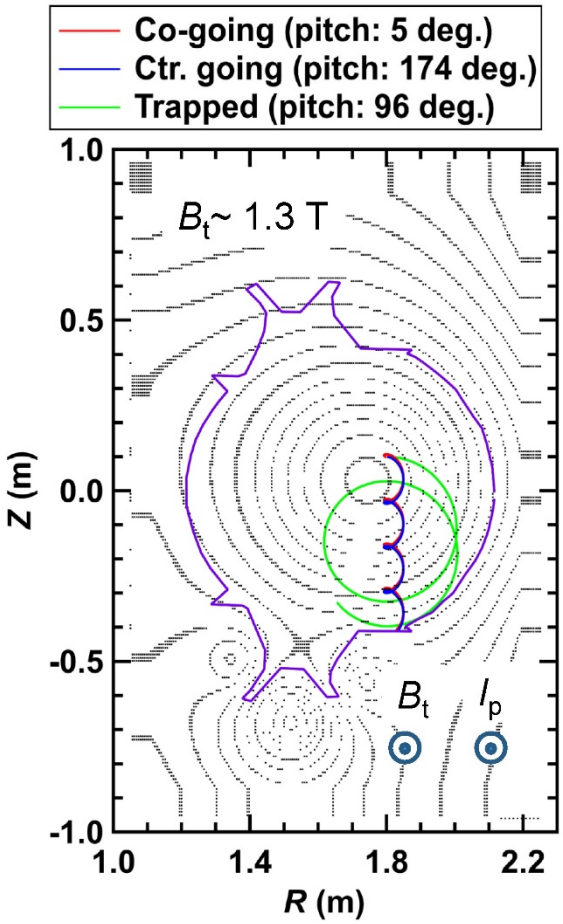


Fig. 4 Typical 1 MeV triton orbit in HL-2A with an $I_p$ of 160 kA.

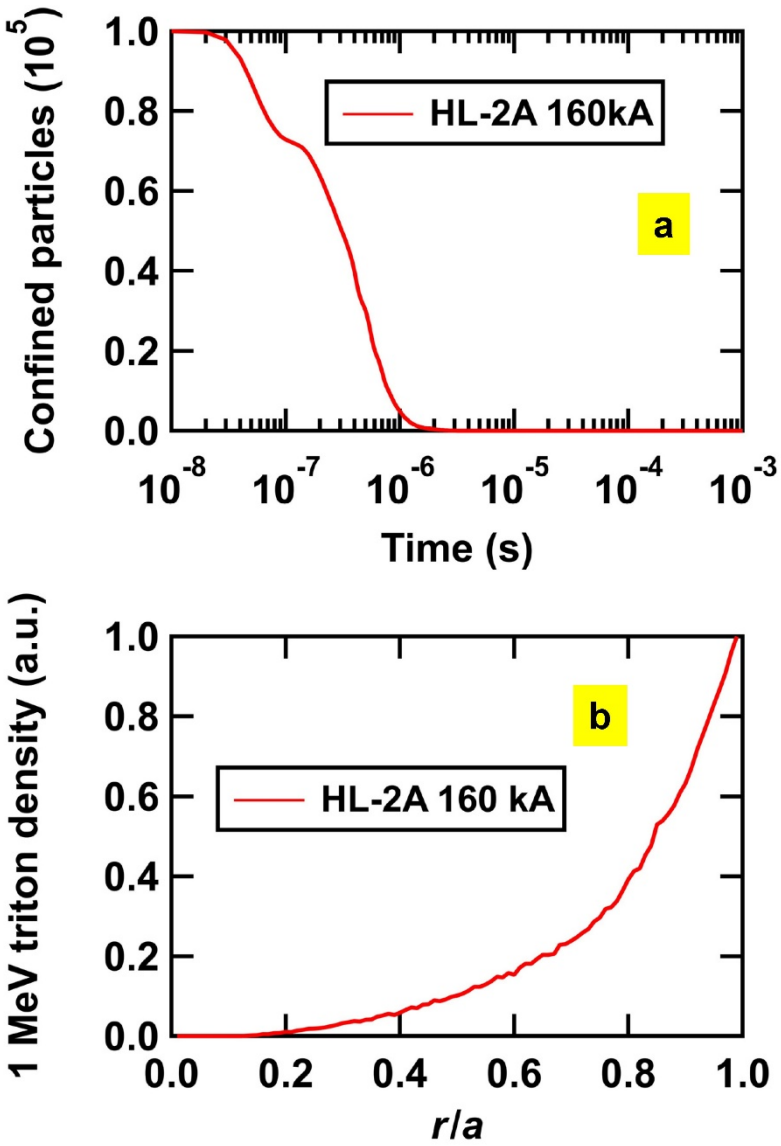


Fig. 5 (a) Time evolution of the number of confined 1 MeV tritons in the HL-2A with the line-averaged density of 2 x $10^{19}$ $m^{-3}$. (b) The radial profile of 1 MeV triton density inside HL-2A, as deduced by the LORBIT code.

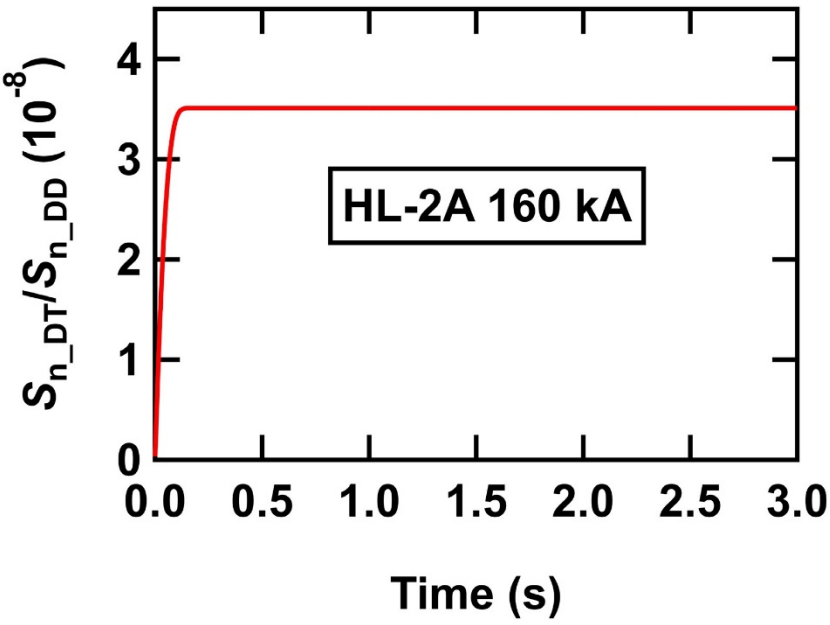


Fig. 6 Time evolution of $S_{n\_DT}/S_{n\_DD}$ calculated by the FBURN code with the line-averaged density of 2 x $10^{19}$ $m^{-3}$.

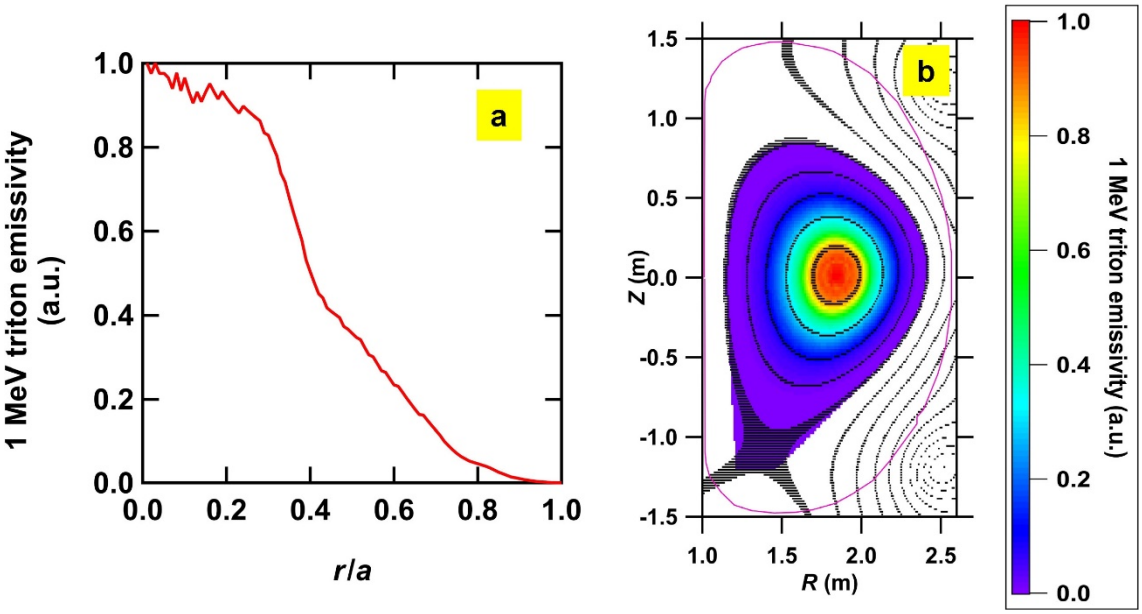


Fig. 7 (a) Radial profile of 1 MeV triton emissivity calculated by the NUBEAM code in the HL-2M with $I_p$ values of 1 MA with the line-averaged density of 2 x $10^{19}$ $m^{-3}$. (b) Two-dimensional plot of the birth profile of a 1 MeV triton used in HL-2M, as adopted by the LORBIT code.

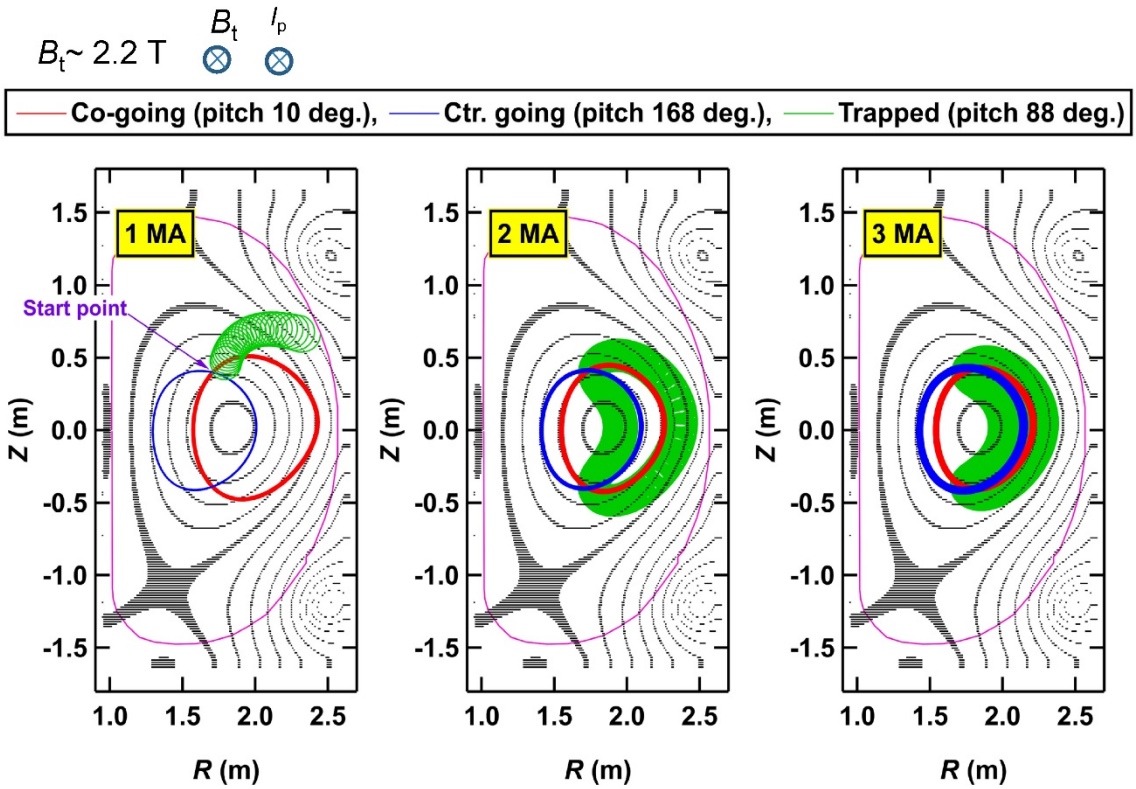


Fig. 8 Typical 1 MeV triton orbit in HL-2M with $I_p$ values of 1 MA, 2 MA, and 3 MA.

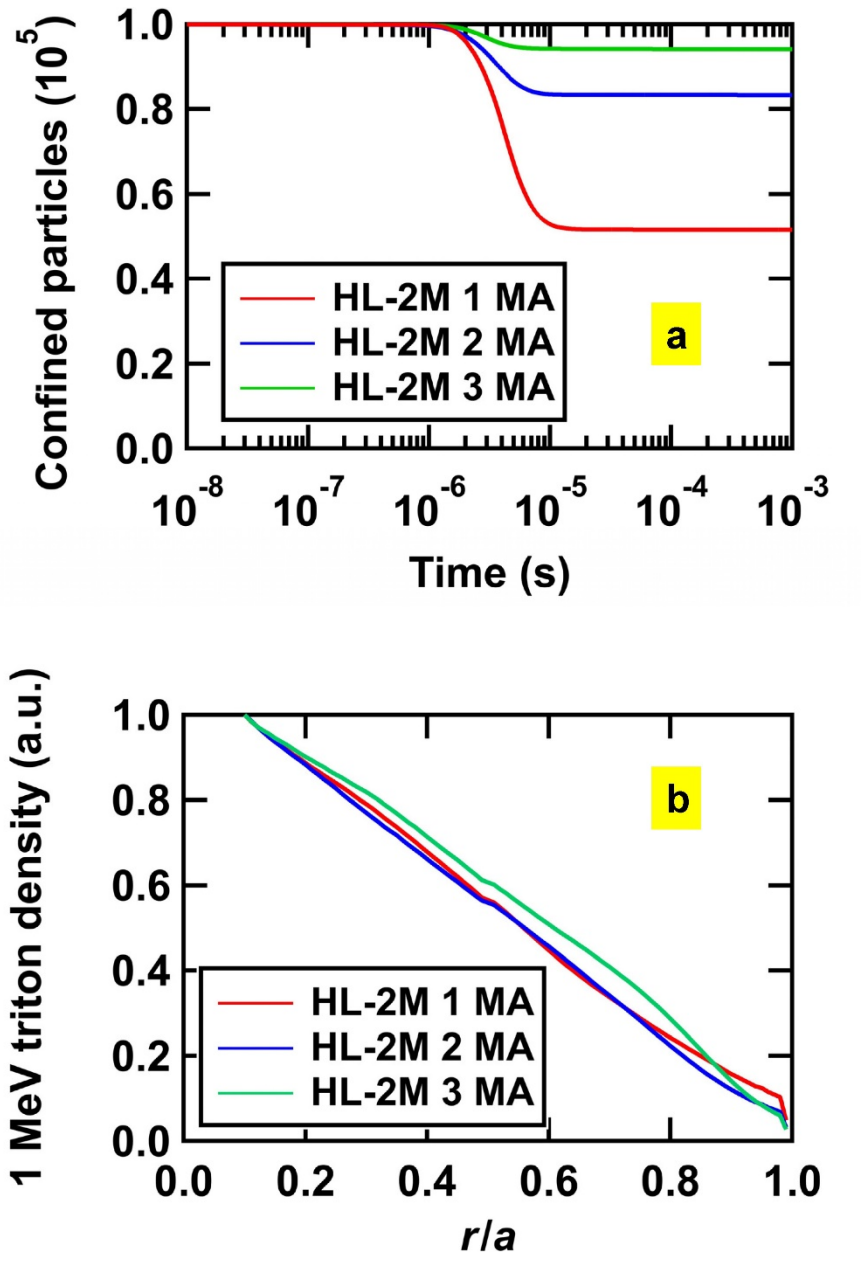


Fig. 9 (a) Time evolution of the number of confined 1 MeV tritons in HL-2M with the line-averaged density of 2 x $10^{19}$ $m^{-3}$. (b) The radial profile of 1 MeV triton density in HL-2M is deduced by the LORBIT code.

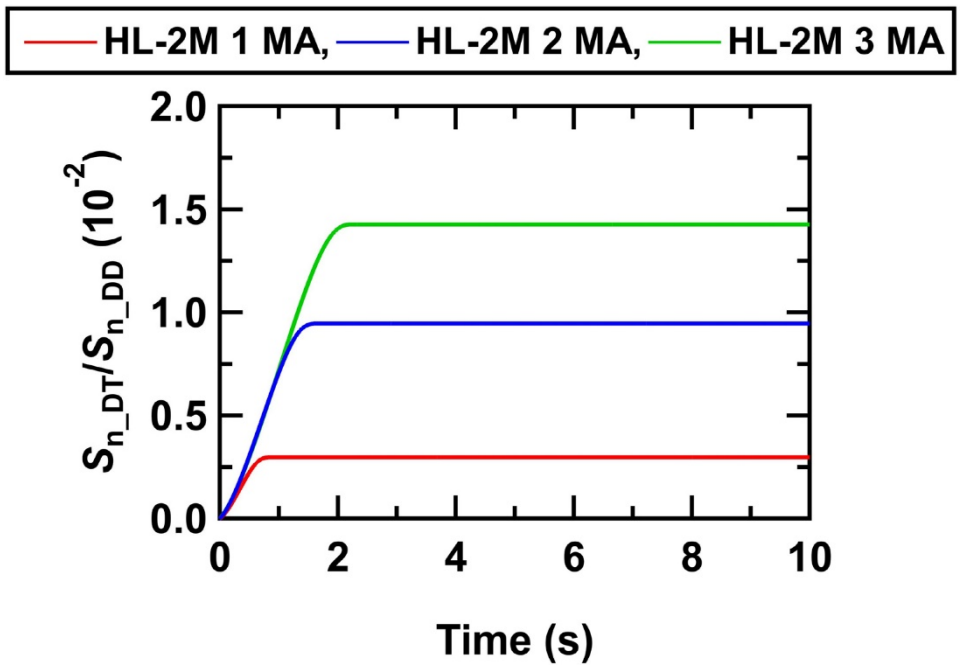


Fig. 10 Time evolution of $S_{n\_DT}/S_{n\_DD}$ calculated by the FBURN code with the line-averaged density of 2 x $10^{19}$ $m^{-3}$.

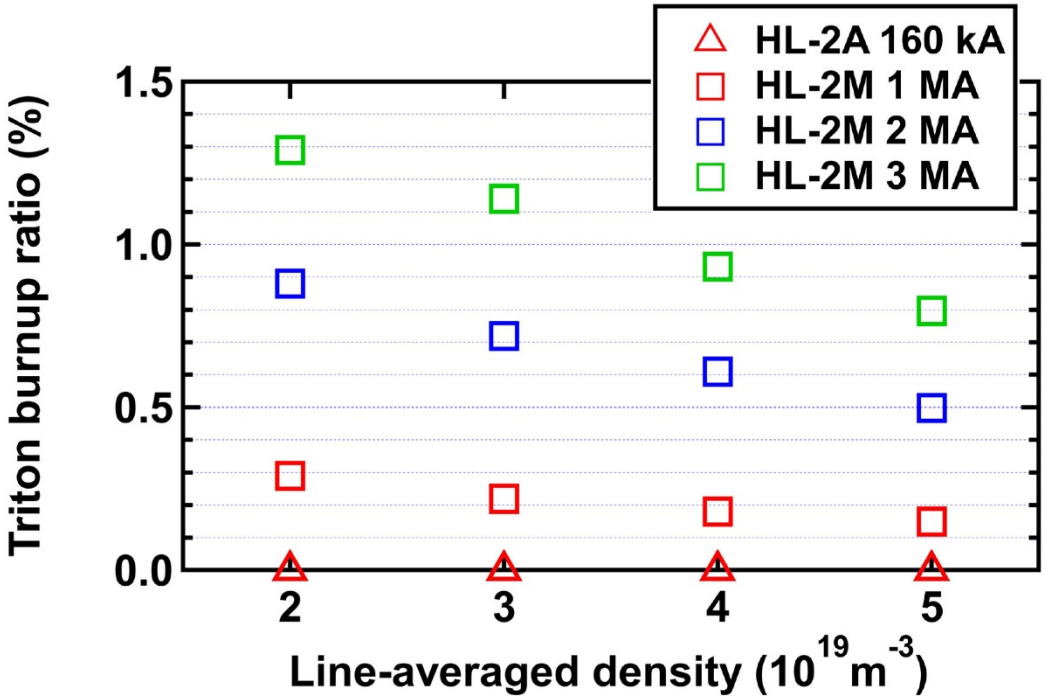


Fig. 11 Triton burnup ratio evaluated in this analysis as a function of line-averaged density.